Journal of Catalysis **202,** 220–228 (2001)
doi:10.1006/jcat.2001.3272, available online at http://www.idealibrary.com on IDEAL®

The Effect of Chromium on Sulfur Resistance of Pd/HY–Al_2O_3 Catalysts for Aromatic Hydrogenation

Linjie Hu,*,[1] Guofu Xia,* Lianglong Qu,* Mingfeng Li,* Can Li,† Qin Xin,† and Dadong Li*

**Research Institute of Petroleum Processing, SINOPEC, Beijing 100083, China; and †State Key Laboratory of Catalysis, Dalian Institute of Chemical Physics, Chinese Academy of Sciences, Dalian 116023, China*

Received December 4, 2000; revised March 14, 2001; accepted May 8, 2001; published online August 9, 2001

Sulfur is a major poison to noble metal catalysts for deep aromatic hydrogenation in the petroleum refining industry. In order to study the sulfur resistance of Pd-based catalysts, a series of Pd, Cr, and PdCr catalysts supported on HY–Al_2O_3 were studied by NH_3-TPD, pyridine-adsorption IR, TPR, IR spectra of adsorbed CO, and toluene hydrogenation in the presence of 3000 ppm sulfur as thiophene under the following conditions: 533–573 K, 4.2 MPa, and WHSV 4.0 h^{-1}. Cr has no influence on the acidity of the catalysts. TPR patterns and *in situ* IR spectra of adsorbed CO revealed a strong interaction between Cr and Pd, and the frequency shift of linear bonded CO on Pd indicates that the electron density of Pd decreases with the increase of the Cr/Pd atomic ratio. The catalytic performance of Pd, Cr, and PdCr catalysts shows that the sulfur resistance of Pd is strongly enhanced by Cr, and the activity reaches its maximum when the Cr/Pd atomic ratio equals 8. The active phase model "Pd particles decorated by Cr_2O_3" is postulated to explain the behavior of PdCr catalysts. © 2001 Academic Press

Key Words: **palladium; chromium; Y zeolite; alumina; sulfur resistance; toluene hydrogenation.**

1. INTRODUCTION

In recent years, more and more attention has been paid to aromatic hydrogenation in diesel fuel because aromatics lower the combustion efficiency (cetane index) and increase the undesirable emissions from diesel engines (1–3). Noble metal catalysts exhibit high activity for aromatic hydrogenation, but such catalysts are generally sensitive to sulfur poisoning. In recent years, the sulfur resistance of noble metal catalysts has been extensively investigated (1–3).

The sulfur resistance of a noble metal can be enhanced by using an acidic support, such as amorphous SiO_2–Al_2O_3, B_2O_3–Al_2O_3, or acidic zeolites (4–11). Many researchers believe that the high sulfur resistance of Pt or Pd on acidic supports arises from the formation of electron-deficient metal particles, $Mx^{\delta+}$, which result from the interaction of the metal particles with the Brønsted acid sites (12–14). Y-zeolite-supported noble metal catalysts, an important type of industrial catalyst for aromatics hydrogenation, have received increasing attention in recent years (1, 2, 15). Therefore, the support is the combination of Y-type zeolite with alumina for the catalysts studied in the present work.

Another possibility to improve the sulfur resistance of a noble metal catalyst is to alloy the active component with another metal. Because the Pt–Pd alloy on various supports exhibits higher sulfur tolerance than either of the components, many researchers were attracted by this system (1, 2, 7–11). So far nobody can give a satisfactory answer to this question. The different properties of the Pt–Pd system from single Pt or Pd have been generally attributed to alloying effects, i.e., electronic and ensemble effect. However, it is still not clear why Pt–Pd bimetallic catalysts are much more active for aromatic hydrogenation in the presence of sulfur. This is partially because both Pt and Pd are active for hydrogenation, and probe molecules that are frequently used in spectroscopy such as CO can adsorb on both of them. One of the possible explanations is "electron-deficient Pt" resulting from Pt–Pd bimetallic interactions. For example, Navarro *et al.* (8) confirmed a strong Pt–Pd interaction in the bimetallic particles formed, and proposed that the electron-deficient character of platinum (isolated Pt clusters on the Pd surface) is responsible for the strong sulfur resistance of the PtPd samples. In contrast, Fujikawa *et al.* (16) demonstrated that the Pd species dispersed on Pt particles were responsible for the high activity of the Pt–Pd bimetallic catalysts because this structure significantly enhances the intrinsic catalytic activity, and the sulfur resistance is not improved by the Pt–Pd system as compared with that in a single Pt or Pd system.

Few papers dealing with the sulfur resistance of bimetallic catalysts other than Pt–Pd can be found (1, 2). Recently, Fujikawa *et al.* (16) studied the influence of Pd, Re, Sn, Ir, Ni, Mo, Ge, and Pf on the sulfur resistance of Pt catalysts. Unfortunately, no positive effects have been found except for the Pt–Pd system. Our previous findings showed that

---

[1] To whom correspondence should be addressed. Current address: Chemical Physics Department, Fritz-Haber-Institut der Max-Planck-Gesellschaft, Faradayweg 4-6, D-14195 Berlin, Germany. Fax: +49 30 8413 4105. E-mail: hu@fhi-berlin.mpg.de.

0021-9517/01 $35.00

other transition metal elements, such as Cr, W, Ag, etc., also have strong effects on the sulfur resistance of Pd/HY–Al_2O_3 (17, 18). For example, PdCr catalyst exhibits much better sulfur resistance than the single Pd catalyst.

In order to further investigate the strong promoting effect of chromium (or its oxides) on the sulfur resistance of palladium catalysts, a series of PdCr catalysts were studied in this work. The sulfur resistance of catalysts was tested with the mixture of toluene, *n*-hexane, and thiophene (3000 ppm sulfur). The model feed contains a relatively great amount of sulfur, as evidenced by the fact that the catalysts could reach their steady-state activity in a short time. The kinetic studies confirmed the strong promoting effect of chromium (or its oxides) on the sulfur resistance of palladium catalysts, and revealed the optimum ratio of Cr/Pd for the catalyst with the best sulfur resistance. The acidic properties were measured by ammonia temperature-programmed desorption (NH_3-TPD) and IR spectra of adsorbed pyridine. The structure of active metal clusters on the surface was investigated by IR spectra of adsorbed CO and temperature-programmed reduction (TPR) in an attempt to account for the excellent sulfur resistance of PdCr catalysts.

2. EXPERIMENTAL

Catalyst Preparation

The precursor of HY is an NH_4Y (produced by the Changling Catalyst Factory, China Petrochemical Corp., Na 1.2 wt%, $SiO_2/Al_2O_3 = 5$, surface area 610 m^2/g). The precursor of Al_2O_3 used is a pseudo-boehmitic powder (SB powder produced by Condea, surface area 238 m^2/g).

The support was formed by extrusion: 70 g of NH_4Y was mixed with 30 g of Al_2O_3, followed by kneading and extruding, and was finally calcined at 873 K for 2 h. All metal catalysts were supported on the prepared HY–Al_2O_3 (surface area 503 m^2/g, pore volume 0.382 cm^3/g).

Pd and Cr were introduced onto the support by pore volume impregnation. The support was contacted with the solution of Pd $(NH_3)_4Cl_2$ in deionized water, followed by drying at 393 K for 2 h and calcinating at 823 K for 2 h. The Pd catalyst was sequentially impregnated with aqueous solutions containing various amounts of $(NH_4)_2CrO_4$ for 2 h, dried at 393 K for 2 h, and then calcined at 823 K (ramp 2 K/min) for 2 h. For comparison, Cr/HY–Al_2O_3 (2.4 wt% Cr on HY–Al_2O_3) was also prepared by aqueous impregnation of the calcined support with ammonium chromate. The composition and physical properties of the catalysts are listed in Table 1.

TABLE 1

Composition of Catalysts (Support HY–Al_2O_3)

Cat. ID[a]	Pd (wt%)	Cr (wt%)	Cr/pd atomic ratio	Surface area (m^2/g)	Pore volume (cm^3/g)
Pd	0.6	0	0	491	0.38
$PdCr_1$	0.6	0.3	1	482	0.38
$PdCr_2$	0.6	0.6	2	483	0.37
$PdCr_8$	0.6	2.4	8	475	0.35
$PdCr_{16}$	0.6	4.8	16	465	0.31
Cr	0	2.4		481	0.35

[a] The subscript of Cr refers to Cr/Pd atomic ratio.

Catalyst Characterization

NH_3-TPD was performed on a DuPont-961 thermal gravity analysis instrument to measure the amount of acidic sites on the catalysts. The catalyst sample was loaded into a platinum basket and dehydrated at 773 K in flowing N_2 (50 ml/min) for 1 h. After the sample was cooled to 373 K, 10% NH_3/N_2 was introduced onto the catalyst until the weight reached a constant value. The catalyst was then purged in flowing N_2 (50 ml/min) to remove the physisorbed ammonia. The temperature was raised to 923 K with a ramp of 10 K/min while the change of the weight was recorded.

IR spectra of adsorbed pyridine were recorded to distinguish and to measure the two types of acidic sites on the surface, *i.e.*, Lewis and Brønsted acids. The catalyst powder was first pressed into wafers (diameter 14 mm, ca. 20 mg), and pretreated in a vacuum of 10^{-5} Pa at 623 K for 2 h. The background spectra were recorded at 298 K. Next, 40 Pa pyridine was introduced at 298 K and kept for 30 min, and then evacuated at different temperatures. The IR spectra were recorded after outgasing at 473 K, 573 K, and 623 K. All spectra were recorded on a Brucker IFS113V IR spectrometer at 298 K. The reported IR spectra in this paper have been background subtracted.

TPR patterns of Pd, Cr, and PdCr/HY–Al_2O_3 were obtained on an AMI-100 chemisorption instrument produced by Zeton Altamira. The catalyst particles were pretreated at 673 K for 30 min in flowing Ar (40 ml/min) and then cooled to 323 K. The mixture 10% H_2/Ar was introduced into the sample loop at a flow rate of 25 ml/min, and then the temperature was linearly ramped at 10 K/min to 1373 K. The hydrogen consumption was recorded by a thermal conductivity detector.

IR spectra of adsorbed CO were recorded with a Nicolet Impact-410 instrument equipped with an IR cell that allows *in situ* treatments with different gases at temperatures up to 1000 K. The samples were finely ground with an agate mortar, pressed into wafers with a diameter of 15 mm (ca. 30 mg), and then placed into the IR cell. The samples were dried at 773 K in flowing air for 1 h, and then evacuated to 10^{-3}–10^{-4} Pa for surface cleaning. Before FFT-IR measurements, samples were reduced under the same conditions as those of the catalytic tests, except at a H_2 pressure of 0.1 MPa. After the sample was cooled to room temperature in flowing H_2, the cell was evacuated to 10^{-3}–10^{-4} Pa, and 2500 Pa CO was introduced into the cell and maintained for 30 min. The IR cell was evacuated to a pressure of 1 Pa to remove the gas-phase CO, and IR spectra were recorded. In order to better observe the peaks corresponding to bound CO, the spectrum collected before CO adsorption was subtracted from the spectrum after CO adsorption.

Catalytic Performance

The sulfur resistance of the catalyst was tested with a continuous down-flow fixed-bed reactor. The reactor was packed with 1.0 g of catalyst (40–60 mesh) diluted with an inert 40–60 mesh ceramic in a ratio of 1 : 1. The upper and bottom parts were filled with particles of a catalytically inactive ceramic material for preheating and preventing channel effects. Catalysts were firstly reduced at 573 K under 4.2 MPa in flowing hydrogen (>99.9%) for 2 h. After reduction, the catalytic reactions were carried out with a weight hourly space velocity (WHSV) of 4.0 h^{-1} and flowing hydrogen (H_2/toluene mole ratio 40), under 4.2 MPa. The reaction temperature was in the range of 533–573 K. The feedstock was a mixture of toluene and *n*-hexane in a volume ratio of 1 : 1, with a certain amount of thiophene to make the concentration of sulfur 3000 ppm in feed.

Reaction products were analyzed by on-line gas chromatography. Methylcyclohexane (MCH) and dimethylcyclopentane (DMCP) were the main products detected except for traces of cyclohexane, benzene, xylene, and hydrocracking products. The hydrogenation of toluene is assumed to be a pseudo-first-order kinetic reaction. Because H_2 is excessive under our reaction conditions, the following approximate formula can be used to calculate the reaction constant (8, 19):

$$k = -(F_{\mathrm{tol}}/m)\ \ln(1 - X),$$

where k is the reaction constant for toluene hydrogenation ($\mathrm{mol_{tol}} \cdot \mathrm{mol_{Pd}}^{-1} \cdot \mathrm{h}^{-1}$), X is the toluene conversion, F is the flow rate of toluene ($\mathrm{mol_{tol}} \cdot \mathrm{h}^{-1}$), and m refers to the metal atoms per gram of catalyst ($\mathrm{mol_{Pd}} \cdot \mathrm{g_{cat}}^{-1}$).

3. RESULTS AND DISCUSSION

A series of HY–Al_2O_3-supported Pd, PdCr, and Cr catalysts were prepared to study the effects of Cr on sulfur resistance and structure of catalyst. All catalysts, except single Cr, contained 0.6 wt% Pd. In order to find the optimum amount of Cr and make reasonable comparisons, the Cr/Pd atomic ratio was varied from 0 to 16 for these catalysts.

NH_3-TPD and Pyridine Adsorption IR

NH_3-TPD and pyridine adsorption IR, as standard techniques, can provide information on the acidity of industrial catalysts. NH_3-TPD thermal gravimetric derivative curves are reported in Fig. 1. The peak area represents the amounts of desorbed NH_3, and peak position is related to the strength of acidity. A pronounced desorption peak at 420 K and a shoulder at 500–700 K were observed. For all the PdCr and Cr catalyst samples, NH_3-TPD curves are quite similar to that of single Pd/HY–Al_2O_3. This indicated that added Cr had no noticeable effects on amount and strength of acidity.

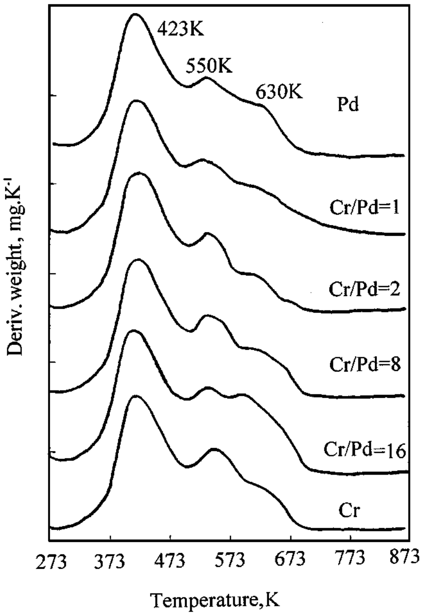

FIG. 1. NH_3-TPD thermogravimetric derivative curves of Pd, PdCr, and Cr supported on HY–Al_2O_3. Cr/Pd atomic ratios are presented.

Pyridine adsorption–desorption IR spectra basically supply information on two types of acidic sites, *i.e.*, Brønsted and Lewis acid. The two bands at around 1450 cm^{-1} and 1540 cm^{-1} are assigned to pyridine molecules adsorbed on Lewis acid and Brønsted acid, respectively. All the catalysts exhibited both Brønsted and Lewis acidity after pyridine desorption at 473–623 K, and amounts of the two types of acidic site are similar for all the prepared Pd, PdCr, and Cr catalysts (Fig. 2). After outgasing at 623 K, pyridine adsorbed on the Brønsted acidic site decreased by 30%, and pyridine on the Lewis acidic site retained constant. This shows that adsorption of pyridine on Lewis acid is stronger than that on Brønsted acid. Generally, the intensity of the signal corresponding to Brønsted sites decreased to a greater extent than that of the Lewis sites upon increasing the outgasing temperature from 473 to 623 K, which means that the latter are stronger than the former. However, the presence of Brønsted sites could be of importance to sulfur resistance of supported Pd catalyst (12–14, 20).

From the measurements of catalyst acidity, it can be concluded that the presence of Cr does not change the acidic properties of the catalysts.

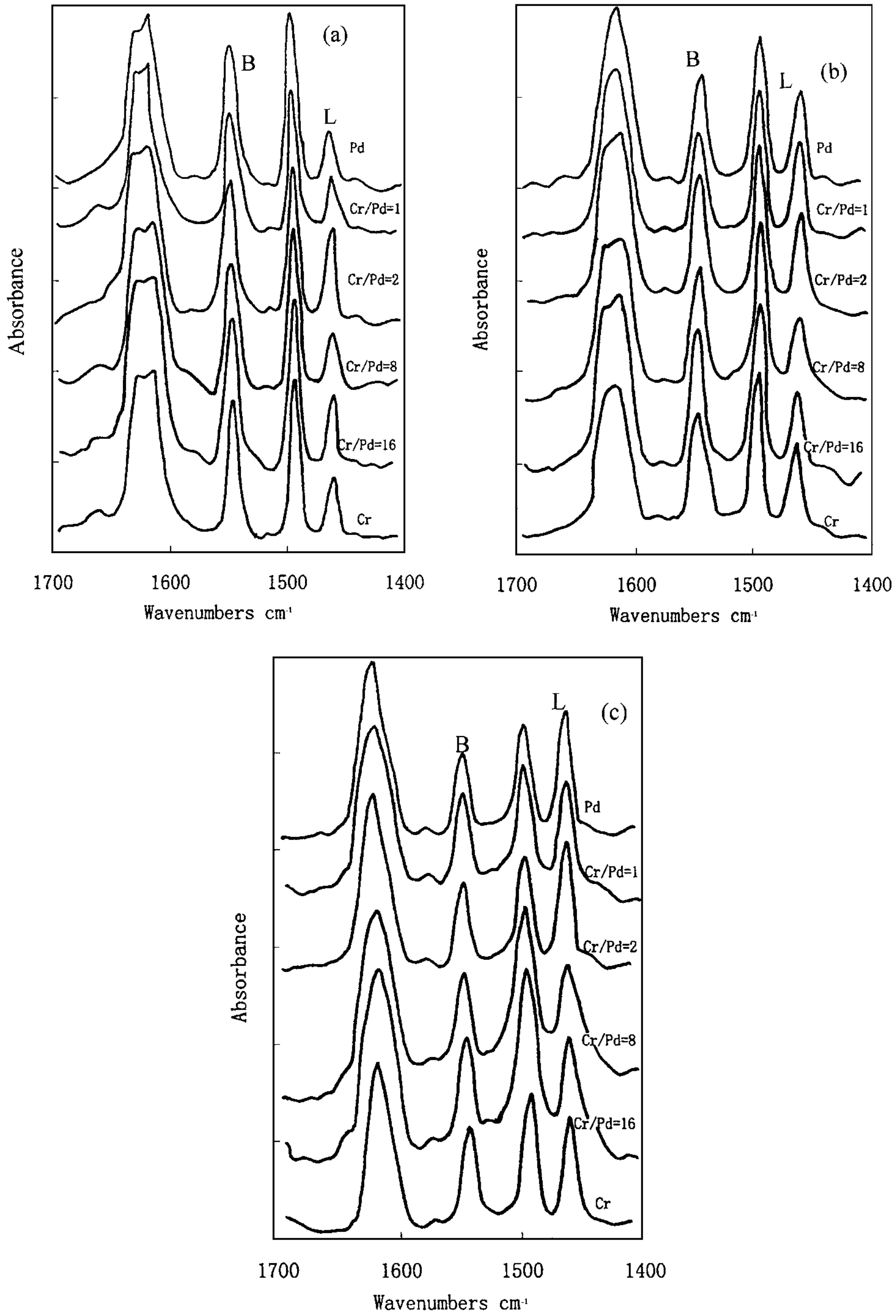

FIG. 2. IR spectra Pd, PdCr, and Cr supported on HY–Al_2O_3 exposed to pyridine vapors, and outgased at different temperatures: (a) 523 K; (b) 573 K; (c) 623 K. Cr/Pd atomic ratios are presented.

Temperature-Programmed Reduction (TPR)

Figure 3 gives TPR patterns of the supported Pd, Cr, and PdCr catalysts. It should be noted again here that all the catalysts had been calcined at 823 K for 2 h after the impregnation. Such a condition is sufficient to decompose the precursors of Cr and Pd, i.e., $(NH_4)_2CrO_4$ and $Pd(NH_3)_4Cl_2$. Therefore, Pd and Cr should exist in the form of oxides on the support before TPR experiments and catalytic performance. The reduction peak of pure Cr catalyst is in the range of 600–750 K as shown in Fig. 3. Therefore, the single Cr catalyst cannot be reduced at all before catalytic performance. For the chromia/Al_2O_3 catalyst, Grünert *et al.* (21) reported the main reduction peak at

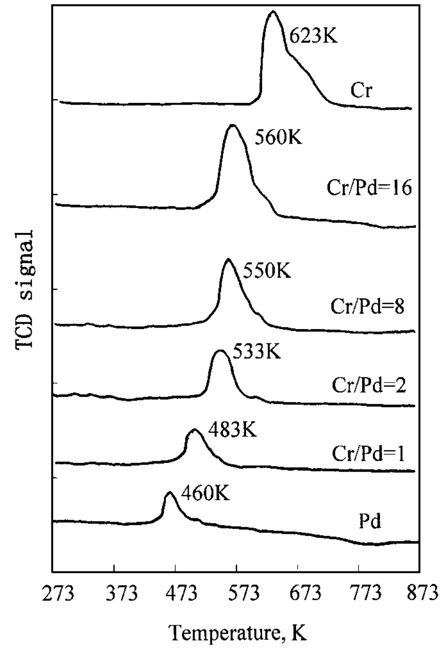

FIG. 3. TPR patterns of Pd, PdCr, and Cr supported on HY–Al_2O_3. Cr/Pd atomic ratios are presented for PdCr catalysts.

approximately 673 K, which is consistent with our results.

Undoubtedly palladium occurs in the form of Pd^0 after reduction before catalytic performance. The TPR profile of the single Pd catalyst showed a peak at 460 K, and the hydrogen consumption ended at 520 K.

For all the PdCr catalysts, only one reduction peak can be seen. The TPR patterns show that the PdCr catalysts reduce in the temperature range between the single palladium and chromium (or its oxides) reductions, indicating that palladium catalyzes the reduction of chromium oxide. This indicated that palladium and chromium (or their oxides) are well mixed or contacted in the fresh catalysts before and after reduction.

As for the oxidation state of chromium on the PdCr catalysts, TPR profiles also can provide some information. As shown in Fig. 3, all the PdCr catalysts show a peak with a maximum lower than 573 K. This peak is shifted toward higher temperatures as the Cr loading increases. For pure chromium oxides, the $T_{\max}$ increases as the Cr loading decreases because of stronger bonding energy between Cr and oxygen (22). These results suggest catalytic reduction of CrOx by palladium. After carrying out calcination in a flow of air at 773 K for 5 h, Grzybowska *et al.* (22) found that chromium is present on alumina in the form of hexavalent species, chromium trioxide, a fraction of which is strongly bound to the support surface. The chromium trioxide on alumina can be reduced to chromium sesquioxide (Cr_2O_3) at relatively low temperatures ca. 523 K, even without the help of Pd (22). Similarly, we can assume most of the chromium on the PdCr catalysts is chromium trioxide after calcination, and the CrO_3 species would first be reduced to chromium sesquioxide during reduction. Only small consumption of H_2 at temperatures higher than 573 K is observed for PdCr catalysts, and no H_2 consumption is observed at temperatures higher than 750 K. It should be noted that the reduction of CrOx is dependent upon the pressure of H_2 and H_2O (22, 23). A relative part of CrO_3 species are probably further reduced to Cr^0 from Cr_2O_3 before activity testing since the catalysts were reduced at much higher H_2 pressure before reaction (4.2 MPa H_2).

CO Adsorption FTIR

Carbon monoxide on metals forms the best studied systems in vibrational spectroscopy, and the C–O stretch frequency is very informative about the direct environment of the molecule (24–26). In order to investigate the structure of metal clusters on catalysts, *in situ* CO adsorption infrared spectroscopy was carried out in this study. Figure 4 shows

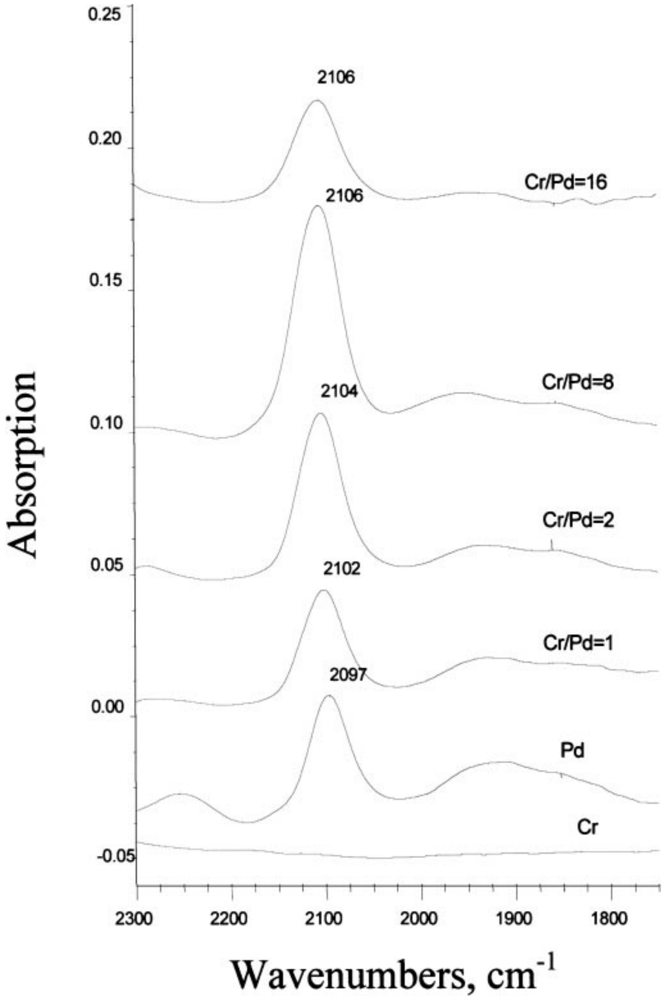

FIG. 4. Transmission IR spectra of CO adsorbed on Pd, Cr and a series of PdCr supported on HY–Al_2O_3. Cr/Pd atomic ratios are presented for PdCr catalysts.

the IR spectra of adsorbed CO on palladium, chromium (or its oxides) and PdCr catalysts supported on HY–Al_2O_3. There are three things to note. The first is the difference in C–O stretching frequency, which reflects the electronic structure of the metal clusters. Second, the IR spectra contain two bands corresponding to linear adsorbed CO (2050–2150 cm^{-1}) and twofold or multifold bonded CO (1800–2000 cm^{-1}). Third, the intensity or area of the adsorption peak represents the amount of adsorbed CO.

A clear absorption peak of linear bonded CO can be seen for all the palladium- containing catalysts, and its frequency is presented in Fig. 4. From TPR profiles, we know pure chromium is present in the form of CrOx under the conditions studied. There was no absorption peak at frequencies between 1800–2200 cm^{-1} for pure chromium, which indicates that CO molecules do not adsorb on CrOx under our conditions. On pure palladium, the linear bonded CO shows a peak at 2097 cm^{-1}. Addition of Cr to Pd leads to a clear shift to higher frequency (blue shift), which shifted to 2106 cm^{-1} for Pd–Cr with an atomic ratio of Cr/Pd 16. The precise absorption frequency depends on CO coverage, geometric effect, and the *d*-electron density of Pd (25, 27).

Due to mutual interactions between the dipoles of the CO molecule, the CO stretch frequency decreases with decreasing coverage (26, 27). The absorbing bands of linear CO bonded on PdCr catalyst should shift to lower frequency. This is because isolation and diminishing of the Pd ensembles by decoration of CrOx and/or Cr^0 decreases the dipole effect of CO, with an effect similar to that of decreasing coverage of CO. This phenomenon was reported for the PdAg/SiO_2 system by Sachtler *et al.* (28, 29). Toolenaar *et al.* (30) proved that the lower frequencies of linear CO on the Pt–Cu alloy were caused by diminished dipole–dipole coupling between adsorbed CO molecules. In contrast, Fig. 4 shows that the linear adsorbed CO frequency increased monotonically with increasing Cr content. According to the π back donation model, the blue shift of CO stretch frequency demonstrates that Pd, which is the only adsorption site of CO for the studied catalyst, exhibits a more “electron-deficient” state in PdCr than that in the single Pd catalyst.

It is also worth noting the relative intensity of the two bands at 2050–2150 cm^{-1} and 1800–2000 cm^{-1} (Fig. 5). It can be seen that the fraction of multibonded CO molecules decreases rapidly with Cr/Pd atomic ratio until it reaches nearly zero at Cr/Pd = 16. This may be explained by a decrease of sites with two or more adjacent Pd atoms as the Cr/Pd ratio increases.

The other interesting point is the strong peak of linear CO on the single Pd catalyst, which seems to be in conflict with the existing reports (27). Freund *et al.* (31) studied CO adsorbed on Pd aggregates deposited on a well-defined alumina model support Al_2O_3/NiAl(110) using infrared spectroscopy. They found that CO is preferentially bridge-bonded on Pd at 300 K, i.e., the population of linear bonded CO is near zero. Other researchers reported a similar conclusion on well-ordered Pd single crystals (27, 32). However, as reported by some other researchers (33–36), a sharp band at about 2080 cm^{-1} is one of the features of IR spectra of adsorbed CO on Pd powder catalyst. This is related to the particle size of palladium on such a catalyst. The industrial support HY–Al_2O_3, with a very large surface area (503 $m^2 . g^{-1}$), is very different from the model catalysts. Compared with the deposition of 2.2 Å Pd (average thickness) on Al_2O_3/NiAl(110) in Ref. (31), our Pd catalyst corresponds to only 0.01 Å Pd on the surface. For our catalyst Pd/HY–Al_2O_3, the strong linear CO peak reveals that Pd particles are very small and/or have a rough surface, which leads to a distance that is too large to be bridge-bonded by CO molecules.

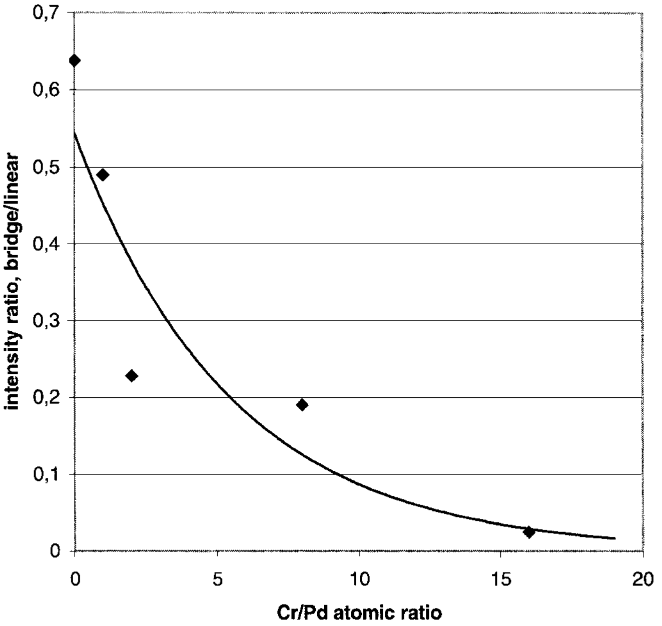

FIG. 5. Ratio of integrated intensities of the adsorption bands for bridge and linear bonded CO for PdCr catalysts as a function of Cr/Pd atomic ratio.

Tests of Sulfur Resistancy

Toluene hydrogenation over Cr, Pd, and PdCr supported on HY–Al_2O_3 was investigated in a continuous down-flow reactor with a mixture of toluene, *n*-hexane, and thiophene. The pseudo-first-order rate constants are reported in Fig. 6, and there is no toluene conversion over the single Cr catalyst under these conditions. It can be seen that the activity was strongly affected by chromium (or its oxides), and such effects become stronger at higher reaction temperatures. For instance, at 573 K, the rate constant is 388 $mol_{tol} . mol_{Pd}^{-1} . h^{-1}$ on single Pd, reaches its maximum of 946 $mol_{tol} . mol_{Pd}^{-1} . h^{-1}$ for PdCr catalyst when Cr/Pd = 8,

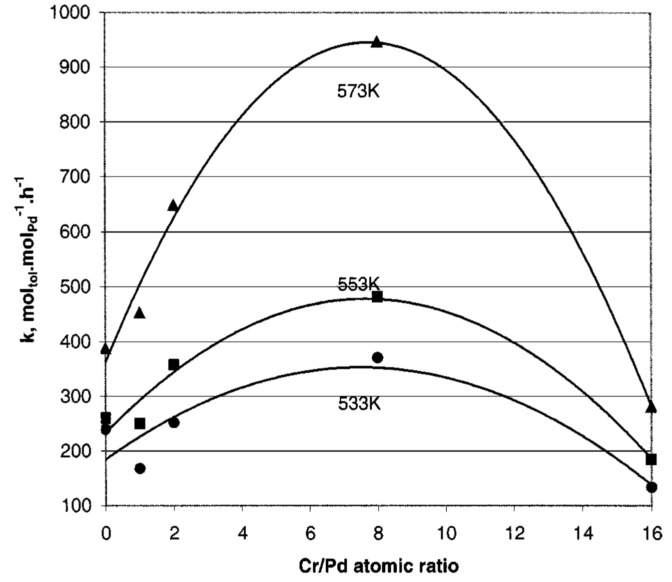

FIG. 6. Pseudo-first-order rate constants for toluene hydrogenation on Pd and PdCr/HY–Al_2O_3 catalysts with various Cr/Pd atomic ratios. Reaction conditions: $P = 4.2$ MPa, WHSV $= 4.0\ h^{-1}$, $T = 533$–573 K, with 3000 ppm sulfur in feed as thiophene.

and then decreases to 281 $mol_{tol} \cdot mol_{Pd}^{-1} \cdot h^{-1}$ when the Cr/Pd atomic ratio is increased further to 16. The activity of toluene hydrogenation is an indicator for sulfur resistance of Pd catalysts. Therefore, we can conclude that proper amounts of chromium (or its oxides) improve the sulfur resistance of Pd/HY–Al_2O_3.

Although the rate constants were obtained at different temperatures in this paper, the activation energies of toluene hydrogenation on these catalysts cannot be calculated on the basis of the results. Sulfur poisoning of metals, or sulfur adsorption on metal surfaces, is dependent on temperature (37), e.g., exposed palladium atoms are related to the reaction temperature. Thermodynamic studies proved that sulfur adsorption on metals is reversible, and partially adsorbed sulfur will desorb as H_2S from metal surfaces with the increase of temperature. For the following equation:

$$\ln(k) = -E_a/RT + \ln(A).$$

The pre-exponential factor A is relevant to active sites, which mainly refers to accessible Pd atoms here. Hence the pre-exponential factor will not remain constant at different temperatures. However, a constant A is prerequisite to get a reasonable activation energy by this equation. Navarro and Fierro *et al.* (8) studied toluene hydrogenation on PtPd/SiO_2–Al_2O_3 with sulfur-containing feed (1200 ppm sulfur as thiophene), and the calculated activation energy is 129.2 kJ/mol. In this case, the increase of the rate constant includes the contribution of A, which would make the calculated activation energy deviate to a high value. In fact, Rahaman and Vannice (38, 39) investigated the kinetic behavior of toluene hydrogenation over palladium supported on various supports. They found that the activation energy remained essentially constant at 49.3 kJ/mol despite large differences in activities, support, and reduction temperatures. As we deduced, the value is much smaller than 129.2 kJ/mol as calculated by Navarro *et al.* (8).

Sulfur-Resistant Mechanism of PdCr Catalysts

To understand the sulfur resistance of PdCr catalysts, the structure of the active phase and the electronic structure of Pd should be considered.

Since single Cr is not active under our reaction conditions, the active phase should contain Pd atoms. TPR results indicate the coexistence of $Cr^{3+}Ox$ (Cr_2O_3) and Cr^0 with Pd^0 on the PdCr catalysts. As far as the formation of PdCr bimetallic particles is concerned, Renouprez and co-workers (40–42) studied PdCr catalysts prepared from a mixed salt palladium chromate using XRD and EXAFS. Palladium chromate was reduced between 473 and 873 K in flowing hydrogen. Below 673 K, Pd particles supported on amorphous CrOx are observed. An EXAFS experiment at the Pd K-edge was performed on the sample reduced at 673 K, which indicates that part of the chromium oxide is reduced and is in close interaction with palladium. Only above 673 K, a bimetallic compound is formed corresponding to the composition $Pd_{88}Cr_{12}$ (40). Therefore, in the case of our PdCr catalysts after reduction, palladium particles seem to comprise the main active phase, which is in close interaction with Cr_2O_3 and/or metallic Cr. PdCr alloy or bimetallic particles are probably not formed in our case.

The palladium particles tend to be coated by the oxide phase (Cr_2O_3) at reduction temperatures below 673 K (40). Since the formation PdCr bimetallic particles is improbable, the coating by Cr_2O_3 is certainly responsible for the increase of the fraction of linear-adsorbed CO, and the apparent palladium area loss for $PdCr_{16}$, which is observed in Fig. 4.

The electron deficiency of palladium particles should be attributed to Cr_2O_3 on the Pd surface or the interface between the oxide phase and metal particles. Primet *et al.* (43) studied the catalytic properties of CrPd/alumina in the combustion of methane in the presence of H_2S. In the case of the fresh catalyst, palladium participates in a strong interaction with the chromium-containing phase (Cr^{3+} or Cr_2O_3), and electron density of palladium can be withdrawn by such species (43). In contrast, theoretical calculation shows that the alloying of Pd with Cr (such as Pd_3Cr and PdCr) results in an electron transfer from Cr to Pd because Cr is more electropositive (44).

Correlated with characterization results, the catalytic performance of supported Pd, Cr, and PdCr catalysts indicates that the sulfur resistance is dependent upon the electronic structure of Pd. The electron-deficient Pd will weaken the

Pd–S bond because sulfur atoms act as electron acceptors (13, 45). As a result of the decrease of sulfur adsorption on surface Pd atoms, more Pd sites are provided for catalyzing toluene hydrogenation.

On the other hand, many articles reported that electron-deficient palladium is much more active in aromatics hydrogenation (46). For toluene hydrogenation, TOF over Pd/SiO_2–Al_2O_3 is 204 compared with 15 over Pd/MgO and 34 over Pd powder (38). Therefore, it is possible that the high sulfur resistance is partially due to high intrinsic activity of Pd for PdCr catalysts.

The hydrogenation activity of PdCr catalysts passes through a maximum at a Cr/Pd ratio of 8, indicating that the Cr/Pd atomic ratio has an optimum value. It is not difficult to explain by the block effect of CrOx coating on the surface of Pd particles. From the CO adsorption infrared spectroscopy in Fig. 4, the differences in frequency of terminal bonded CO became less and less pronounced, but the intensity of total CO absorption bands decreased rapidly with the increase of the Cr/Pd atomic ratio from 8 to 16. The apparent activity would decrease when the block effect of CrOx exceeds its contribution to the sulfur resistance of Pd particles.

4. SUMMARY

Pd, PdCr, and Cr catalysts supported on HY–Al_2O_3 were prepared to investigate the sulfur resistance of the PdCr catalysts. Although the single chromium (or its oxides) catalyst is not active for toluene hydrogenation under the studied conditions, kinetic studies showed that a PdCr catalyst with the optimum Cr/Pd ratio exhibits much higher hydrogenation activity than a single palladium catalyst with the same palladium content. The findings make some sense in the development of industrial catalyst for deep aromatic reduction of diesel fuel.

TPR patterns and IR spectra of adsorbed CO indicate the strong interaction between Pd and CrOx, and the formation of palladium particles probably coated by CrOx after reduction. CrOx species enhance the "electron-deficient" properties of palladium particles. Because the acidity of the catalyst does not change with the addition of Cr, as shown by NH_3-TPD and IR spectra of adsorbed pyridine, the significant enhancement in sulfur resistance of Pd by CrOx can be attributed mainly to the "electron-deficient" Pd particles. On the other hand, since palladium particles are coated by Cr_2O_3, more palladium atoms would be "buried" by chromium oxide with the increase of the chromium content. Therefore, the apparent activity of PdCr catalysts goes through a maximum at about Cr/Pd = 8, where the pseudo-first-order rate constant for toluene hydrogenation increased by a factor of 2.4 from that over single Pd at 573 K.

ACKNOWLEDGMENTS

The authors thank Dr. Günther Rupprechter and Dr. Javier Giorgi at Fritz-Haber-Institut der Max-Planck-Gesellschaft for their helpful discussions.

REFERENCES

1. Cooper, B. H., and Donnis, B. B. L., *Appl. Catal. A: General* **137**, 203 (1996).
2. Stanislaus, A., and Cooper, B. H., *Catal. Rev.-Sci. Eng.* **36**, 75 (1994).
3. Song, C. S., *Chem. Tech* **29**(3), 26 (1999).
4. Corma, A., Martinez, A., and Martinez, S. V., *J. Catal.* **169**, 480 (1997).
5. Reyes, P., Fernandez, J., Pecchi, G., and Fierro, J. L. G., *J. Chem. Tech. Biotech.* **73**, 1 (1998).
6. Bergen, H., Blekkan, E. A., and Holmen, A., *Hydrotreatment Hydrocracking Oil Fractions* **106**, 391 (1997).
7. Yasuda, H., Sato, T., and Yoshimura, Y., *Catal. Today* **50**, 63 (1999).
8. Navarro, R. M., Pawelec, B., Trejo, J. M., Mariscal, R., and Fierro, J. L. G., *J. Catal.* **189**, 184 (2000).
9. Micheaud-Especel, C., Bazin, D., Guerin, M., Marecot, P., and Barbier, J., *React. Kinet. Catal. Lett.* **69**, 209 (2000).
10. Fujikawa, T., Idei, K., and Usui, K., *Sekiyu Gakkaishi* **42**(4), 271 (1999).
11. Yasuda, H., Kameoka, T., Sato, T., Kijima, N., and Yoshimura, Y., *Appl. Catal. A: General* **185**, L199 (1999).
12. Sachtler, W. M. H., and Stakheev, A. Y., *Catal. Today* **12**, 283 (1992).
13. Dalla Betta, R. A., and Boudart, M., *in* "Proceedings, 5th International Congress on Catalysis, Palm Beach, 1972" (J. W. Hightower, Ed.), Vol. 2, p. 1329. North Holland, Amsterdam, 1973.
14. Dalla Betta, R. A., Boudart, M., Gallezot, P., and Weber, R. S., *J. Catal.* **69**, 514 (1981).
15. Arias, P. L., Cambra, J. F., Guemez, B., Barrio, V. L., Navarro, R., Pawelec, B., and Fierro, J. L. G., *Fuel Processing Technol.* **64**, 117 (2000).
16. Fujikawa, T., Idei, K., Ebihara, T., Hirofumi, M., and Usui, K., *Appl. Catal. A: General* **192**, 253 (2000).
17. Hu, L., Nie, H., Qu, L., Xia, G., Shi, Y., and Li, D., *in* "Proceedings of the American Chemical Society 217th National Meeting, March 1999," Part 1, 026-FUEL. Am. Chem. Soc., Washington, DC, 1999.
18. Hu, L., Xia, G., Qu, L., Li, C., Xin, Q., and Li, D., *J. Mol. Catal. A: Chemical* **171**, 169 (2001).
19. Huang, T. C., and Kung, B. C., *Ind. Eng. Chem. Res.* **34**, 1140 (1995).
20. Hu, L., Li, D., Qu, L., Shi, Y., and Xia, G., *Acta Petrolei Sinica (Petroleum Processing Section)* **15**, 41 (1999).
21. Grünert, W., Saffert, W., Feldhaus, R., and Anders, K., *J. Catal.* **99**, 149 (1986).
22. Grzybowska, B., Sloczynski, J., Grabowski, R., Wcislo, K., Kozlowska, A., Stoch, J., and Zielinski, J., *J. Catal.* **178**, 687 (1998).
23. Mac Iver, D. S., and Tobin, H. H., *J. Phys. Chem.* **64**, 451 (1960).
24. Niemantsverdriet, J. W., "Spectroscopy in Catalysis-An Introduction." VCH, New York, 1993.
25. Yates, J. T., *Surf. Sci.* **300**(1–3), 731 (1994).
26. Chabal, Y. J., *Surf. Sci. Rep.* **8**, 211 (1988).
27. Hoffmann, F. M., *Surf. Sci. Rep.* **3**, 107 (1983).
28. Soma-Nato, Y., and Sachtler, W. M. H., *J. Catal.* **32**, 315 (1974).
29. Primet, M., Mathieu, M. V., and Sachtler, W. M. H., *J. Catal.* **44**, 324 (1976).
30. Toolenaar, F. J. C. M., Reinalda, D., and Ponec, V., *J. Catal.* **64**, 110 (1980).
31. Wolter, K., Seiferth, O., Kuhlenbeck, H., Baeumer, M., and Freund, H. J., *Surf. Sci.* **399**, 190 (1998).

32. Ortega, A., Hoffmann, F. M., and Bradshaw, A. M., *Surf. Sci.* **119**, 79 (1982).
33. Eischens, R. P., Pliskin, W. A., and Francis, S. A., *J. Chem. Phys.* **22**, 1786 (1954).
34. Eischens, R. P., Francis, S. A., and Pliskin, W. A., *J. Phys. Chem.* **60**, 194 (1956).
35. Clarke, J. K. A., Farren, G., and Rubalcava, H. E., *J. Phys. Chem.* **71**, 2376 (1967).
36. Angevaare, P. A. J. M., Hendrickx, H. A. C. M., and Ponec, V., *J. Catal.* **110**, 11 (1988).
37. Bartholomew, C. H., Agrawal, P. K., and Katzer, J. R., *Adv. Catal.* **31**, 135 (1982).
38. Rahaman, M. V., and Vannice, M. A., *J. Catal.* **127**, 251 (1991).
39. Rahaman, M. V., and Vannice, M. A., *J. Catal.* **127**, 267 (1991).
40. Borgna, A., Moraweck, B., and Renouprez, A., *J. Chim. Phys.* **86**, 1719 (1989).
41. Borgna, A., Moraweck, B., Massardier, J., and Renouprez, A. J., *J. Catal.* **128**, 99 (1991).
42. El Hamdaoui, A., Bergeret, G., Massardier, J., Primet, M., and Renouprez, A., *J. Catal.* **148**, 47 (1994).
43. Khairulin, S., Beguin, B., Garbowski, E., and Primet, M., *J. Chem. Soc., Faraday Trans.* **93**, 2217 (1997).
44. Delbecq, F., Verite, l., and Sautet, P., *Chem. Mater.* **9**, 3072 (1997).
45. Gallezot, P., Datka, J., Massardier, J., Primat, M., and Imelik, B., *in* "Proceedings, 6th International Congress on Catalysis, London, 1976" (G. C. Bond, P. B. Wells, and F. C. Tompkins, Eds.), Vol. 2, p. 696. The Chemical Society, London, 1977.
46. Karpinski, Z., *Adv. Catal.* **37**, 45 (1990).